Large scale fire test

Large scale fire test: the development of a travelling fire in open ventilation conditions and its influence on the surrounding steel structure

Ali Nadjai[1], Naveed Alam[1], Marion Charlier[2], Olivier Vassart[2], Stephen Welsh[3], Antoine Glorieux[2], Sjostrom Johan[4]

ABSTRACT

In the frame of the European RFCS-TRAFIR project, natural fire tests in large compartment were conducted by Ulster University, involving steel structure and aiming at understanding the conditions in which a travelling fire develops, how it behaves and impacts the surrounding structure. During the experimental programme, the path and geometry of the travelling fire was studied and temperatures, heat fluxes and spread rates were measured. The experimental data is presented in terms of gas temperatures recorded in the test compartment at different positions and levels. The influence of the traveling fire on the surround structure is presented in terms of the temperatures recorded in the selected steel columns and beams. The scope of the experimental work is extended using CFD modelling with FDS software, which demonstrate a good agreement with measurements. The temperatures in the test compartment were dependent on the positioning of the travelling fire band as well as the height from the floor level. The non-uniform temperatures in the compartment lead to transient heating of the nearby structural steel elements, resulting in a reduction of their resistance which may influence the global structural stability. The results obtained will help to understand the behaviour of travelling fires and their influence on the structural members. This knowledge will help to reduce the travelling fire associated risks in future.

Keywords: Travelling fire tests; Natural fire tests; Steel Structure; Large-scale compartment tests; CFD Modelling

1 INTRODUCTION

The response of a structure subjected to fire is dependent on the fire exposure conditions. Small compartment fires behave in a relatively well understood manner, usually defined as a post-flashover fire where the temperatures within the compartment are considered uniform. However, with modern architecture there is an increase of open large-floor plan spaces, for which the assumption of post-flashover fire does not

hold and there is instead a smaller localised fire that moves across the floor with time. The current fire exposure conditions were developed using extrapolation of existing fire test data. The existing data comes from small compartment tests for which a uniform distribution of gases and temperatures fits well. In case of large compartments, this assumption of uniform temperatures does not hold. Travelling fires have been observed and investigated in several structural failures especially from 2000 onwards: The World Trade Centre Towers [3] in New York City in 2001, the Windsor Tower [4] in Madrid in 2005, and the Faculty of TU Delft Architecture building [5] in Netherlands in 2008. From the detailed investigations conducted on such fire events that occurred over the last two decades in large compartments, it is understood that such fires have a great deal of non-uniformity. They generally burn locally and move across floor. This phenomenon generates non-uniform temperatures in the compartment and transient heating of the surrounding structure. This type of fire scenario is idealized as the travelling fire [1,6].

Although majority of the fire exposure scenarios provided in the design codes consider uniform temperatures within the compartment, there is also some guidance available related to non-uniform temperatures. In the EN1991-1-2 [2], two models are provided which consider a non-uniform temperature distribution: the localised fire model and the advanced fire models (zone models and computational fluid dynamic models). Nevertheless, the localised fire method considers a static fire which does not translate the effect of a travelling fire. For zone models, the situation starts as a two-zone model which is based on the assumption of accumulation of combustion products in a layer beneath the ceiling, with a horizontal interface. Uniform characteristics of the gas may be assumed in each layer and the exchanges of mass, energy and chemical substance are calculated between these different zones [2]. Although this model considers a non-uniform temperature distribution within the compartment, it does not translate the travelling nature of a fire. The CFD (computational fluid dynamic) models enable to solve numerically the partial differential equations giving in all points of the compartment, the thermo-dynamic and aero-dynamic variables. These models are consequently complex and imply a high computational cost. The recent years have seen growing interest in investigating travelling fires which underlined the inadequacy of uniform heating in large compartments [7-14]. Further research efforts are needed, especially to extend the experimental data related to such fire scenarios which is scarce, limited, and partial.

2 THE EXPERIMENTAL PROGRAMME

During the experimental programme, three large-scale fire tests were conducted in a compartment with different ventilation conditions having similar fire load. The compartment was a representative of a modern office layout and was used for travelling fire tests multiple times. Detailed instrumentation was employed during the tests. This paper provides the details of the first fire test which was conducted with open ventilation conditions.

2.1 Details of the Test Structure

The floor plan between the outer gridlines of the test structure was 15 m x 9 m while the level of the ceiling from the floor finish surface was 2.90 m as shown in Figure 1 (b). The test compartment is a representative of a modern office building and represents a part of an open layout office building. The structure was made of steel beams and columns as the main structural frame while hollow-core precast slabs were used for the construction of ceiling, Figure 1 (a). A solid concrete wall was built along one of the shorter sides while 1.0 m down-stands were provided along the longer dimensions of the test compartment as seen in Figure 1 (b) and (c).

The structural steel frame of the test compartment was built by Saverfield Ltd, local partner to FireSERT. The steel columns were separated into two categories, the structural columns, and the dummy columns. The structural columns were part of the main structural steel frame while the dummy columns were only provided for data acquisition purposes. All columns were fixed to the pre-existing reinforced concrete flooring via anchorage bolts. The structural columns were fixed to the concrete floor using four anchorage bolts. All the structural columns were 3.5 m extended beyond the roof. The connections between the structural columns and beams were designed as fin-plates. The distance between the structural columns along the longer direction of the test compartment was 5.0 m while the same along the shorter direction was 3.0 m. The structural frame was laterally restrained using four diagonal bracings, two each along the longer and the shorter directions.

(a)

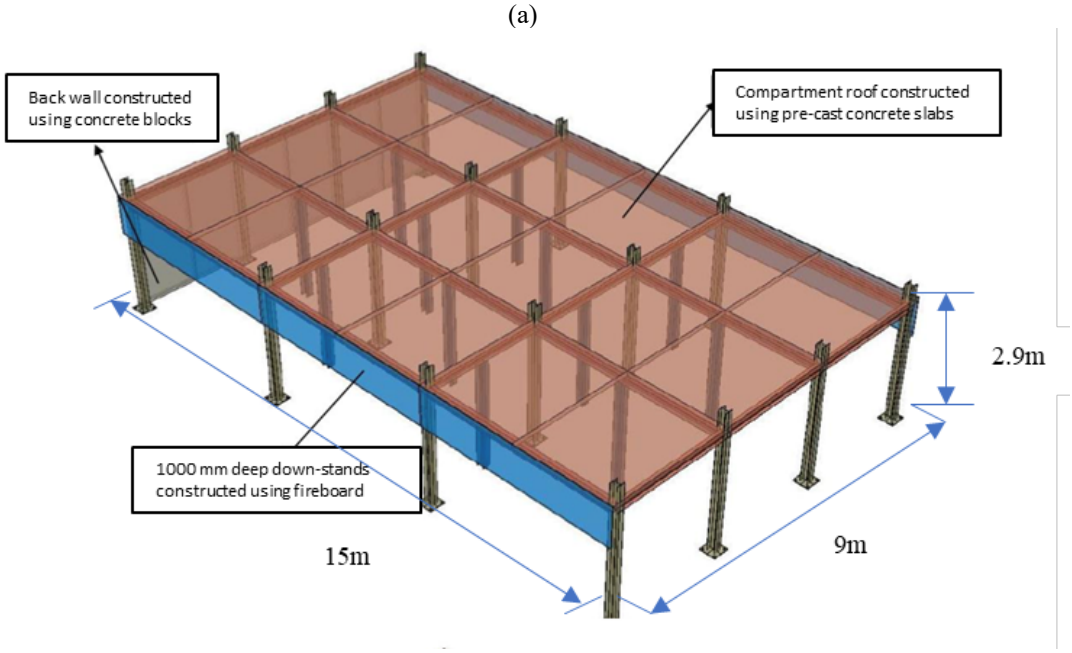

(b)

(c)

Figure 1: Details of the test structure: (a) Structural steel frame and concrete slabs: (b) Schematic view of the test compartment: (c) Test compartment with 1 m down stands

The dummy columns provided for data acquisition purposes were erected between the concrete floor and the roof beams. The dummy columns were fixed to the floor and the bottom flange of the beams using two anchorage bolts. The steel used for the construction of the test compartment (including the dummy columns) was grade S355. Both the structural and dummy columns, as well as the beams provided along the longer direction of the test compartment, consisted of HEA 200 hot rolled steel sections (see Table 1). On the other hand, the beams in the shorter direction consisted of HEA 160 hot rolled steel sections. The roof of the test compartment consisted of 120 mm thick hollow-core precast concrete slabs which were provided along the shorter direction of the compartment. As the test compartment was intended to be used for multiple fire tests, the structural columns of the steel frame were protected using intumescent coating (R60) in order to maintain the structural integrity during the fire tests. It is seen in Figure 2 (b) and (c) that only the structural columns were protected while the dummy columns are kept unprotected for data acquisition purposes. A summary of the steel frame used for the test is given in Table 1.

Table 1: Summary of the steel frame and fire protection details

Description	Sections	Section Factor (m^{-1})	Length Height (m)	Protection Applied
Structural columns	HEA 200	211	3.5	Yes: R60
Dummy columns	HEA 200	211	2.7	No
Long beams	HEA 200	174	4.8	No
Short beams	HEA 160	192	3.0	No

2.2 Details of the Fire Load

The fuel load used for the travelling fire tests was determined to be a representative of an office building following the recommendations of the Eurocode 1 [2]. As the test compartment was representative of an office building, Eurocodes provide a medium fire growth rate (t_α = 300 seconds) and a fire load density of 511 MJ/m^2 for such occupancies. In the frame of TRAFIR-RFCS project, Gamba et al. [11] performed a series of fire tests with uniformly distributed cellulosic fire loads, aiming at defining an arrangement representative of an office building according to Eurocode 1. This work led to devise a well-established methodology, used to define the fuel load for the experimental campaign described in this paper. To achieve a medium fire growth rate for the office building and reach a fire load density of 511 MJ/m^2, 9 layers of wooden sticks with an axis distance of 120 mm (90 mm intervals) were provided in three different

directions. The wood sticks were 30 mm wide and 35 mm deep. The first layer of the wooden sticks was laid at 60° angle while the second layer was laid at an angle of 120°. The third layer was at 0° or 180° and the process was repeated in such a way the 6th layer of the sticks laid at 0° or 180° had a lateral offset of 60 mm with respect to the third layer as shown in Figure 2 (b) and (c). The final layer (the ninth layer) of the fuel wood was at 0° or 180°, such an arrangement helped to visually observe the travelling behaviour of fire from one stick to another. The fuel load arrangement was kept the same during all three tests while the ventilation conditions were varied from one test to another.

The fuel wood source consisted of the species "*Picea abies*" with an average density 470 kg/m^3 having a moisture content of 15.22%. The fuel wood was provided along the centre of the test compartment. The fire load was 14 m long stretching along the longer dimension of the test compartment. For convenience, a gap of 500 mm was maintained between the walls and the edge of the fuel bed at both ends as seen in Figure 2 (a). The width of the fuel bed was 4.2 m and was aligned with the centre line of the compartment. Such an arrangement of the fire load resulted in a distance of 2.4 m from the edge of the fuel bed to the centreline of the columns provided along in the longer dimension along gridline Ⓐ and Ⓓ. The wood sticks were provided on a platform constructed using concrete blocks and gypsum fireboards as shown in Figure 2 (b) and (c). The platform was at height of 325 mm from the concrete floor finish level. The point of ignition was selected at mid-width of the fire load and was located at 0.5 m from its edge, i.e., at a distance of 1 m from the back wall and at a distance of 2.1 m from the edges of the fuel bed along the longer direction.

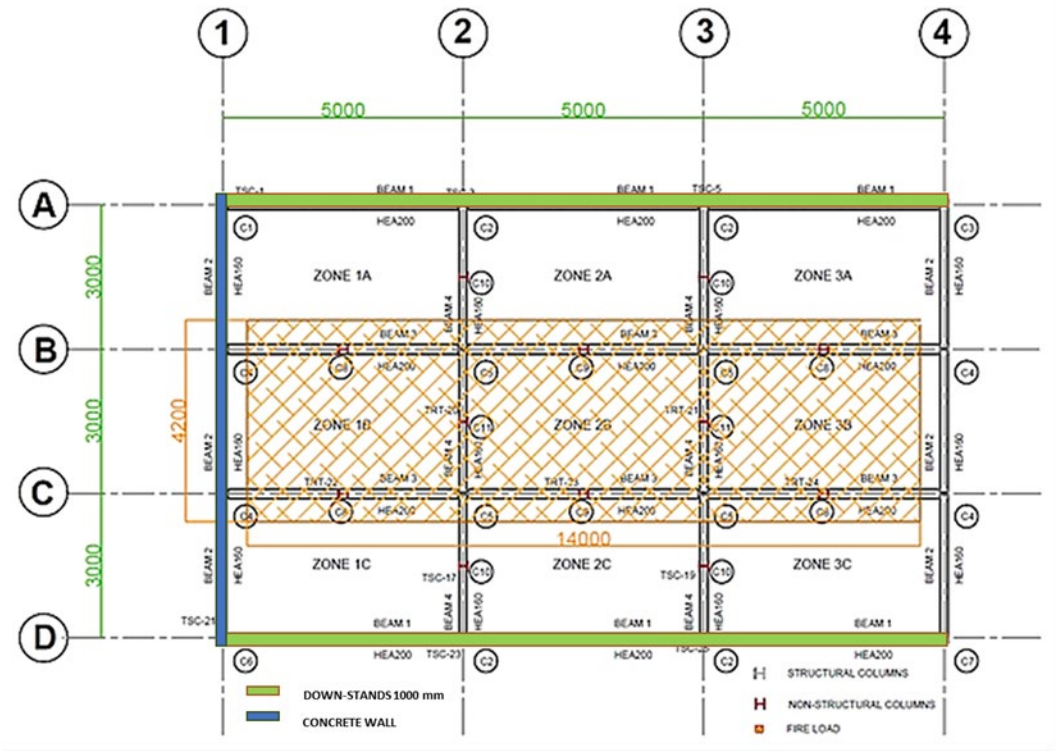

(a)

(b)

(c)

Figure 2: Fuel load arrangement and steel columns: (a) Schematic view of fuel wood: (b) fuel wood provided in the test compartment: (c) Front view of fuel wood

2.3 Details of the Instrumentation

The purpose of these large-scale tests was to investigate the dynamics of the travelling fire and to record fire related data. The recorded data during the test included the compartment temperatures, temperatures in the structural steel components, the heat fluxes, and the mass loss of the wooden fuel. For data acquisition purposes, intensive instrumentation was applied, which consisted of thermocouples, heat flux gauges, thin-skinned calorimeters, anemometer, and the load cells. Details of the instrumentation are provided in the following sections.

2.3.1 The Temperature recordings

The gas temperatures in the compartment were recorded using thermocouples provided at different levels as an individual sensor and in groups as thermocouple trees. The details of the thermocouple positioning are shown in Figure 3 (a). In this paper, details of the thermocouples provided along the centreline of the test compartment have been provided. The thermocouples along the centreline of the test compartment were provided using five thermocouple trees, TRL-4 through TRL-8 in Figure 3 (a) represent these thermocouple trees. The first thermocouple tree, TRL-4, was positioned at 1.5 m from the back wall while the remaining thermocouple trees, TRL-5 through TRL-8 were positioned at 2.5 m intervals All five trees were equipped with six thermocouples at different levels. The positioning of the first thermocouple from the floor finish level was 0.5 m (L1). The thermocouples at levels 2, 3, 4 and 5 were at 1.0 m, 1.5 m, 2.0 m, and 2.5 m respectively. The last thermocouple provided in each tree was at 2.7 m from the floor finish level (L6) as shown in Figure 3 (c). Such arrangement of thermocouples allowed temperature recordings at different locations along the length as well at different heights and levels of the test compartment.

To analyse the influence of the travelling fire on the surrounding steel structure, intensive instrumentation was conducted to record the temperatures in the columns and the beams. Although temperatures were monitored in different columns, details of the instrumentation and recorded temperatures in the dummy columns located along the centreline of the travelling fire have been provided in this article. These columns are identified as C11 in Figure 3 (a) which are adjacent to thermocouple trees TRL-5 and TRL-7. Temperatures in the columns (C11) were monitored at five levels: L1 to L5 as show in Figure 3 (b). Temperatures in the columns at each level were recorded using three thermocouples. Two thermocouples were provided the flanges while the third thermocouple was provided in the web as shown in Figure 3 (d). In total, 15 thermocouples were employed to record the temperatures in each column positioned along the centreline of the test compartment within the fuel wood. These thermocouples have been identified as 1 through 15 in Figure 3 (d).

Temperatures in the steel beams were monitored in the middle adjacent to the thermocouple trees. In this paper, the discussion has been focused on the central beams between gridlines Ⓑ and Ⓒ provided along the gridlines ② and ③. The selected beams are adjacent to thermocouple trees TRL-5 and TRL-7, Figure 3 (a). Temperatures in each beam were monitored via three thermocouples. The first thermocouple was provided

in the bottom flange (B-16) while the second thermocouple was provided in the web (B-17). The last thermocouple in the beams (B-18) was provided in the top flange as shown in Figure 3 (e).

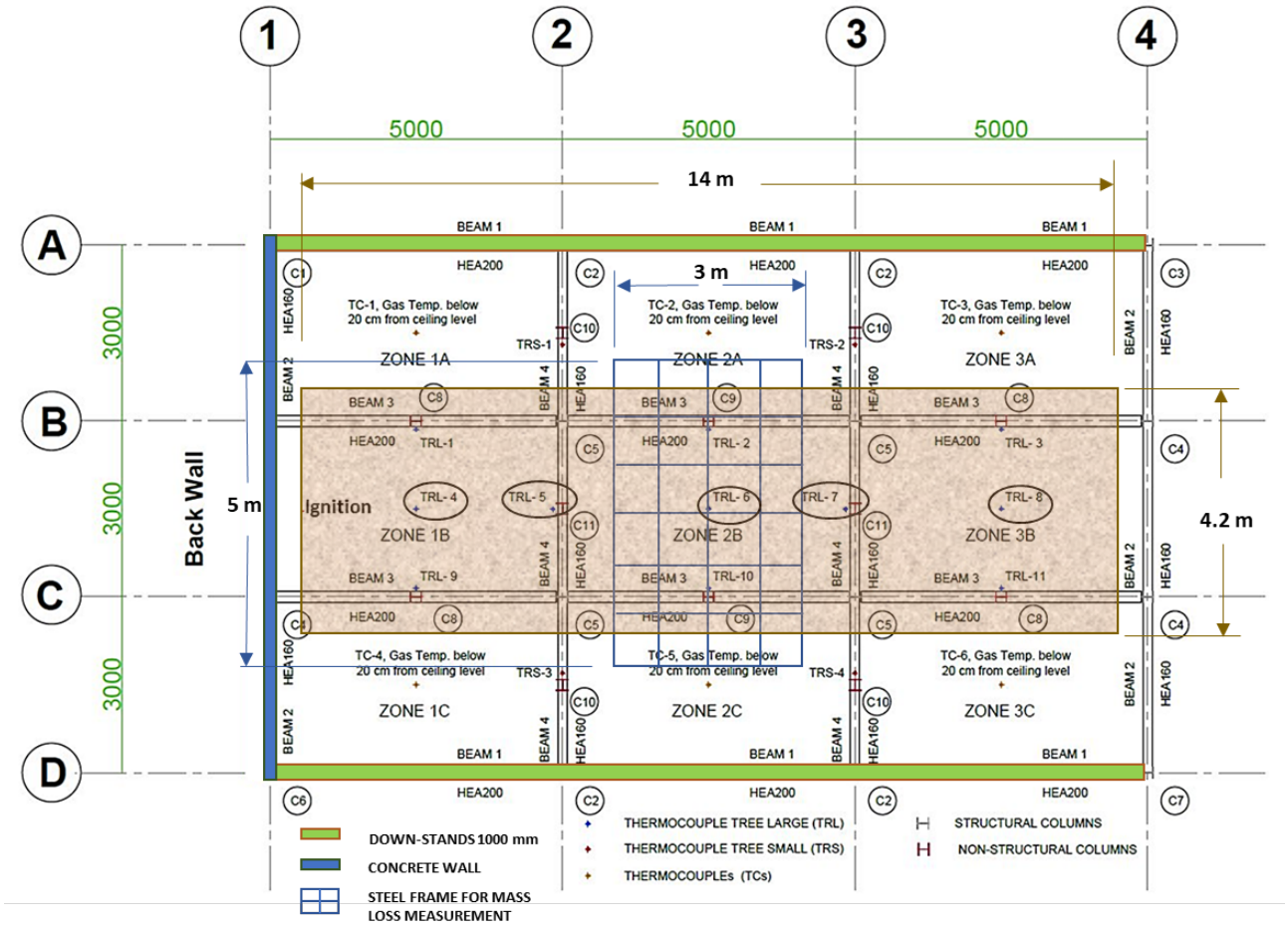

(a)

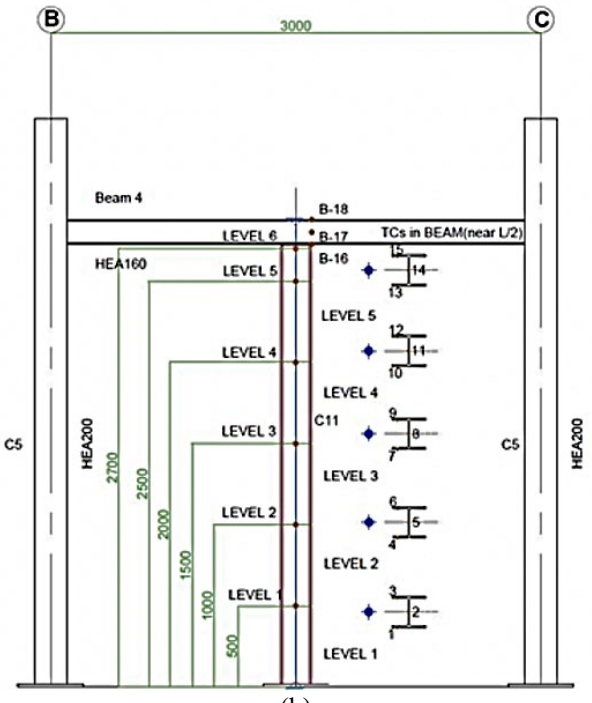

(b)

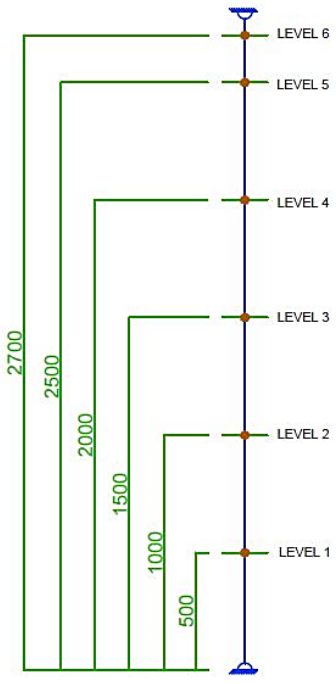

(c)

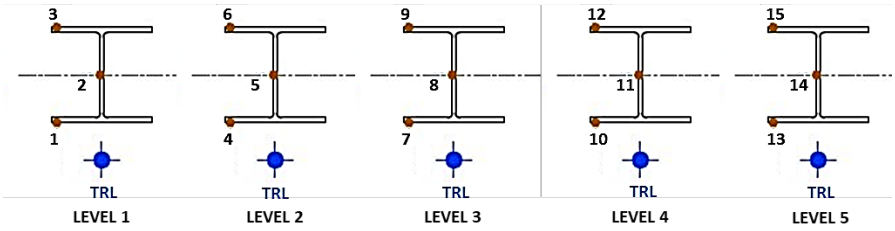

(d)

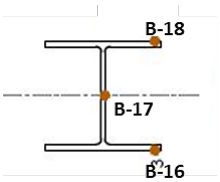

(e)

Figure 3: Details of thermocouples, (a) positioning of thermocouple trees (b) thermocouples in beams and columns, (c) thermocouples in large thermocouple trees; (d) thermocouples in columns, a closer view; (e) thermocouples in beams, a closer view

2.3.2 The Mass Loss Recording

One objective of this experimental work was to record the mass loss of the fuel wood during the travelling fire test. The mass loss of the fuel wood was monitored in the middle of the compartment between gridlines ② and ③ using a steel platform shown in Figure 3 (a). The steel platform was 5 m long x 3 m wide and was supported on four load cells a shown in Figure 4. The load cells were connected to the data acquisition system to record the data. To avoid any damage to the steel platform during the fire tests, fire blanked was wrapped around each part. In addition to the steel platform, the load cells and the cables of the data acquisition system were also protected using the fire blanket as shown in Figure 4. On top of the steel platform, two layers of gypsum fire board were provided to support the fuel wood. The area of gypsum fire boards supporting the fuel load for mass loss recording purposes was 4.2 m x 3.6 m as shown in Figure 3 (a). The top surface of the gypsum fire board layers was at 325 mm distance from the floor finish level, aligned with other fire board panels used to support the fuel wood. Although the fire boards supporting the fuel wood above the steel platform were at the same level from the floor, these were intentionally separated from the rest of the floorboards to ensure accurate measurement of the fuel load during the fire test.

Figure 4: Mass load recording frame with load cells and fire protection arrangements of the steel frame used for mass loss recording

2.3.3 The Data Acquisition System

All the assigned sensors were connected to the data logging system through extension cables. The extension cables were stretched along the roof and were connected with the data loggers stationed in the site office as shown in Figure 5. A layer of fire blanked was provided under these cables to evade any damage from the heat during the test. Due to higher number of sensors applied, multiple data loggers were employed for data recording purposes.

Figure 5: Extension cables for data sensors and data loggers

3 RESULTS AND DISCUSSION

The results from the first travelling fire test are presented in the following:

3.1 The Fire Behaviour

The source of ignition was kept at 1.0 m from the back wall and 0.5 m from the edge of the fuel wood. After ignition, the fire developed and a rise in temperatures was record by the thermocouples closer to the fire. It is seen in Figure 6 (a) that the highest temperatures are recorded by thermocouples provided in TRL-4 while the lowest temperatures are recorded by thermocouples provided in TRL-8. This was evident as the positioning of the travelling fire was closer to the TRL-4 while the remaining thermocouple trees were outside the flames as shown in Figure 6 (b). As the fire travelled ahead, a rise in temperatures were recorded in TRL-5 after 30 minutes from ignition. At this point, temperatures recorded by TRL-4 and TRL-5 were higher as compared to the rest of the thermocouple trees as shown in Figure 6 (c). The positioning of the flames is in between TRL-4 and TRL-5, Figure 6 (d).

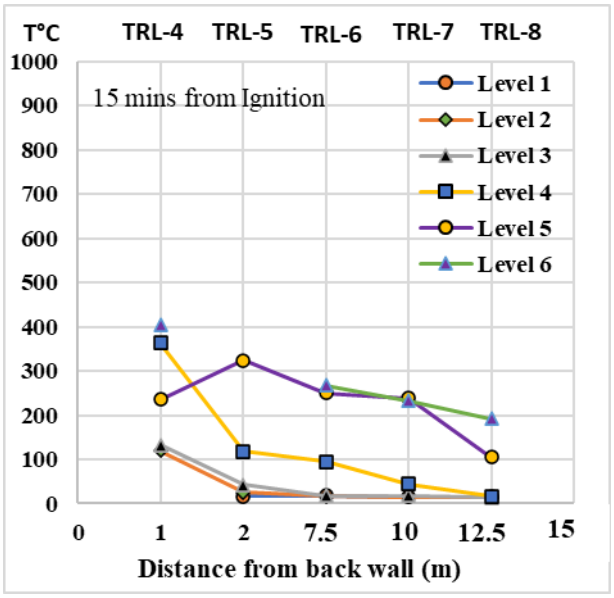
T°C
TRL-4
TRL-5
TRL-6
TRL-7
TRL-8
15 mins from Ignition
Level 1
Level 2
Level 3
Level 4
Level 5
Level 6
1000
900
800
700
600
500
400
300
200
100
0
0
1
2
7.5
10
12.5
15
Distance from back wall (m)

(a)

(b)

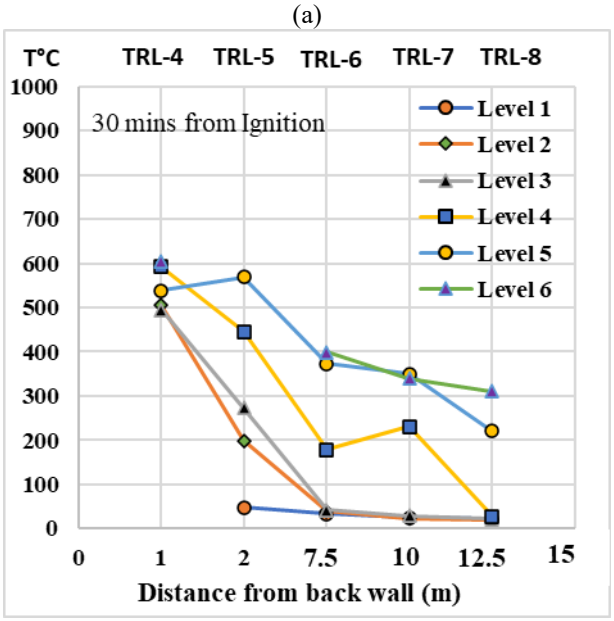
T°C
TRL-4
TRL-5
TRL-6
TRL-7
TRL-8
30 mins from Ignition
Level 1
Level 2
Level 3
Level 4
Level 5
Level 6
1000
900
800
700
600
500
400
300
200
100
0
0
1
2
7.5
10
12.5
15
Distance from back wall (m)

(c)


00 30 07

(d)

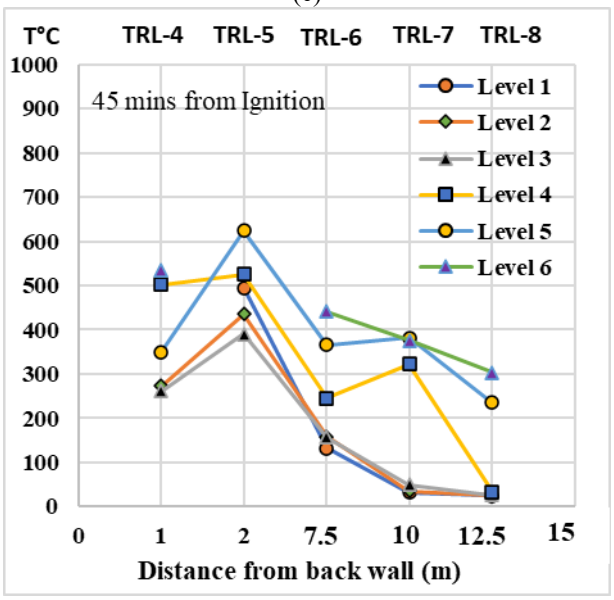
T°C
TRL-4
TRL-5
TRL-6
TRL-7
TRL-8
45 mins from Ignition
Level 1
Level 2
Level 3
Level 4
Level 5
Level 6
1000
900
800
700
600
500
400
300
200
100
0
0
1
2
7.5
10
12.5
15
Distance from back wall (m)

(e)


00 45 05

(f)

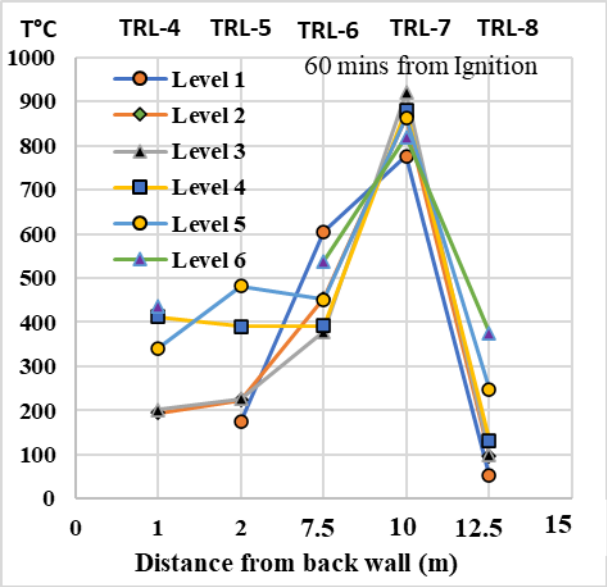

(g)

(h)

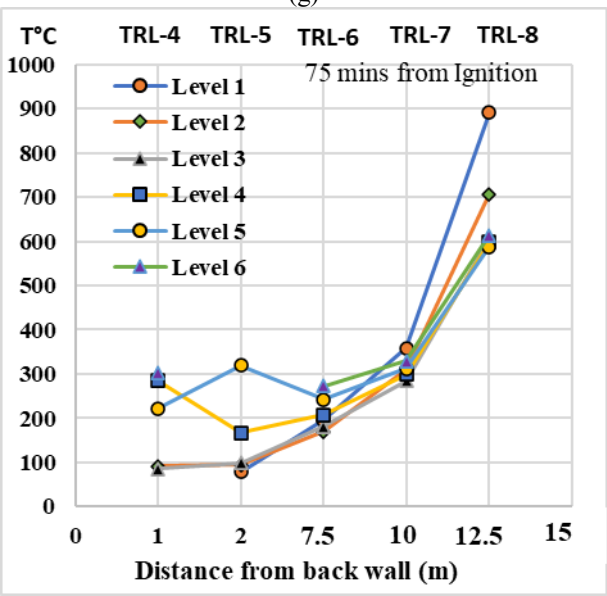

(i)

(j)

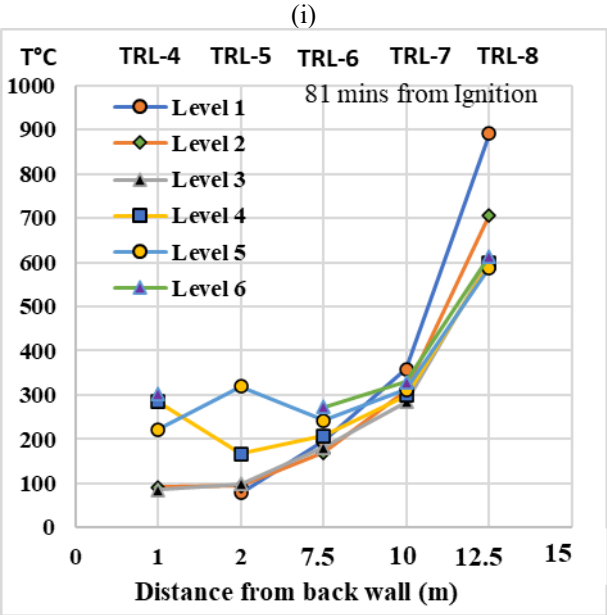

(k)

(l)

Figure 6: Recorded temperatures at different levels and photos; (a) &(b) after 15 mins; (c) & (d) after 30 mins; (e) & (f) after 45 mins; (g) & (h) after 60 mins; (i) & (j) after 75 mins; (k) & (l) after 81 mins

231 The fire continued to travel along the length of fuel bed and got closer to the middle of the compartment
232 after 45 minutes from ignition. This resulted in a decrease of the recorded temperatures at TRL-4 while a
233 small rise in recorded temperatures in TRL-6 was observed as shown in Figure 6 (e). The recorded
234 temperatures are highest at TRL-5 after 45 minutes as this thermocouple tree is engulfed in flames (Figure 6
235 (f)). After 60 minutes from ignition, the fire has got closer to gridline ③, as a result, an increase in the
236 temperatures in TRL-7 has been recorded, Figure 6 (g) and (h). At this point, the temperatures recorded at
237 TRL-8 are still very low. The temperatures recorded at TRL-4 and TRL-5 have reduced significantly and are
238 below 500°C. After 75 minutes from ignition, TRL-8 positioned closer to the fore-end of the test
239 compartment is completely engulfed in fire as seen in Figure 6 (j). This is reflected in the recorded data as
240 highest temperatures are recorded in the compartment at TRL-8 (given in Figure 6 (i)). With the
241 consumption of fuel wood, recorded temperatures in the test compartment reduce except for TRL-8 which is
242 still under the influence of the travelling fire as shown in Figure 6 (k) and (l).
243 The behaviour of the travelling fire was also observed by monitoring the distance between the fire front and
244 the burnout at its back end, along the longer dimension of the test compartment. This distance has been
245 referred to the fire band width in this paper. The maximum band width of the travelling fire observed during
246 the test as well as that observed through videos and pictures of the fire test is given in Figure 7. The
247 "travelling" behaviour of the fire (i.e. when the back end of the fire begins to travel) starts at 28 minutes
248 from ignition for the test. This evolution suggests a fairly constant fire band width of around 3.0 meters,
249 with the lowest value occurring when the fire reaches the central part of the test compartment.
250
251

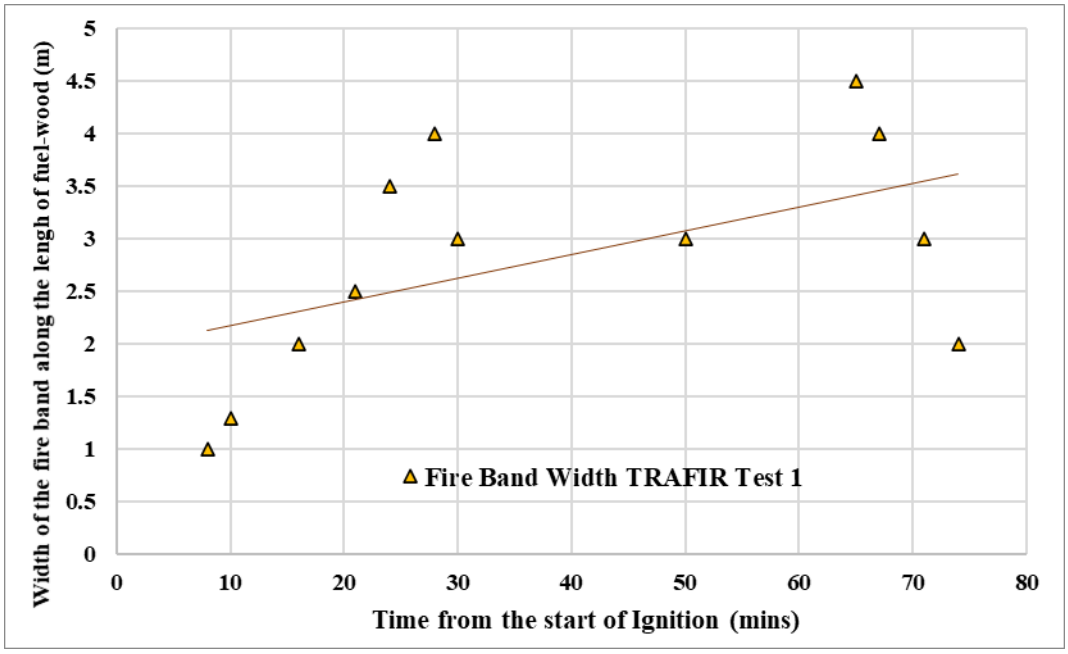

Figure 7: Fire band width at different intervals during the fire

3.2 Gas temperatures recorded in the Test Compartment

The evolution of gas temperatures in the test compartment along the longer dimension, parallel to the travelling fire, are presented in terms of recorded data via thermocouple trees TRL-4 through TRL-8 in Figure 8. The positioning of the thermocouple trees was presented in Figure 3 (a) which shows the first thermocouple tree (TRL-4) positioned in the middle of Zone 1B at 1.5 m from the source of ignition. The remaining thermocouple trees were positioned at 2.5 m centres and were equipped with six thermocouples each as discussed previously. It should be noted that the thermocouple provided at L1 in each thermocouple tree was at 0.5 m from the floor finish level and lies within the fuel load.

The following observations were made during the fire test:

- The gas temperatures recorded in TRL-4 present strong variations. Some extreme values (maximum and minimum) are measured for a very limited period of time (almost instantaneously) and should not be considered when evaluating the global profile of the curve. The TRL-4 also presents a strongly non-uniform temperature distribution along its height (lower temperatures are met for higher levels). Also, it can be seen in Figure 8 (a) that the thermocouple from TRL-4 L1 went deficient at around 30 minutes.
- With the fire band travelling towards the next thermocouple tree (TRL-5), the temperatures recorded at TRL-4 reduce while the temperatures at TRL-5 increase, illustrating the travelling nature of the

fire. Temperatures recorded at TRL-5 reached 900°C after 38 minutes of the ignition. Similarly, the maximum recorded temperatures using TRL-6, TRL-7 and TRL-8 at L2 were 995°C, 975°C and 1000°C after 50 minutes, 57 minutes and 70 minutes from ignition respectively as shown in Figure 8 (b).

- The gas temperatures from TRL-4 & TRL-5 positioned close to the ignition source are globally lower than the ones from other TRL's placed away further in the compartment away from the ignition source. This phenomenon is even more noticeable for upper levels. This could be explained by the fact that at these locations, the fire is in the developing phase for the initial part of the test. Indeed, the fire reaches the entire width of the fuel bed after 23 minutes from ignition and the temperature peaks in TRL-4 after around 20 minutes.
- The curves from TRL-4 & TRL-5 also present a shorter "plateau" of maximum temperatures (i.e. the period of time for which higher temperatures are maintained) as compared to those for other TRL's. For the TRL-4 and TRL-5, a sharper growth and decay are measured, with a short-lasting plateau of around 10 minutes.
- The maximum gas temperatures recorded in TRL-6 to TRL-8 are in the same order of magnitude: around 1000°C.
- During the test, one of the thermocouples malfunctioned at L6, this has been omitted in Figure 8 (f).

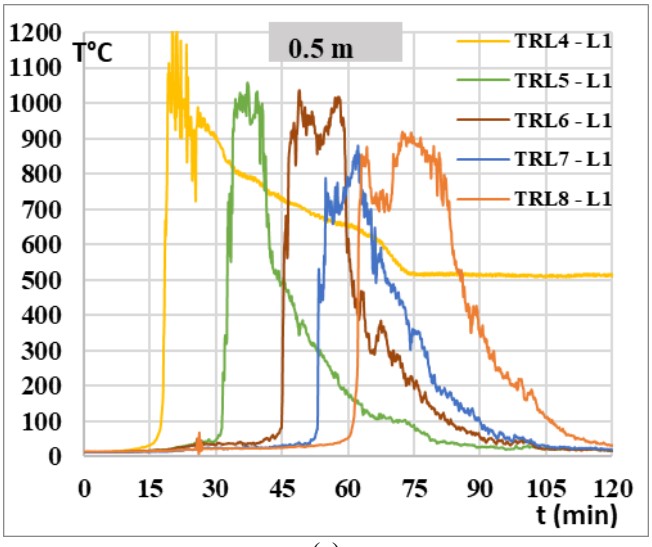

(a)

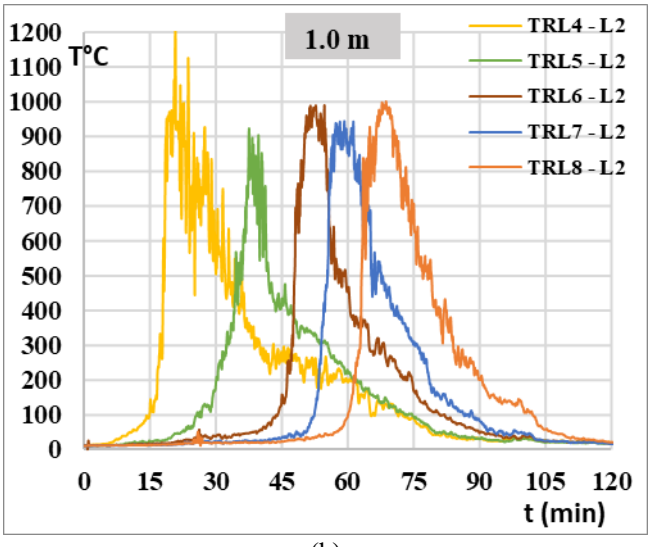

(b)

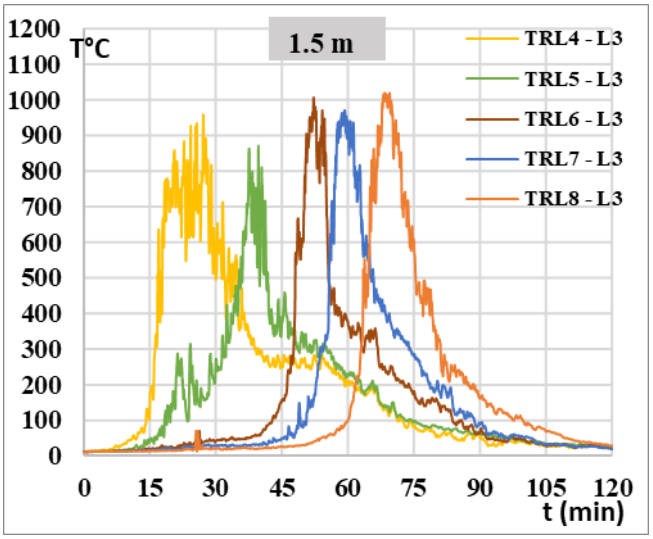

(c)

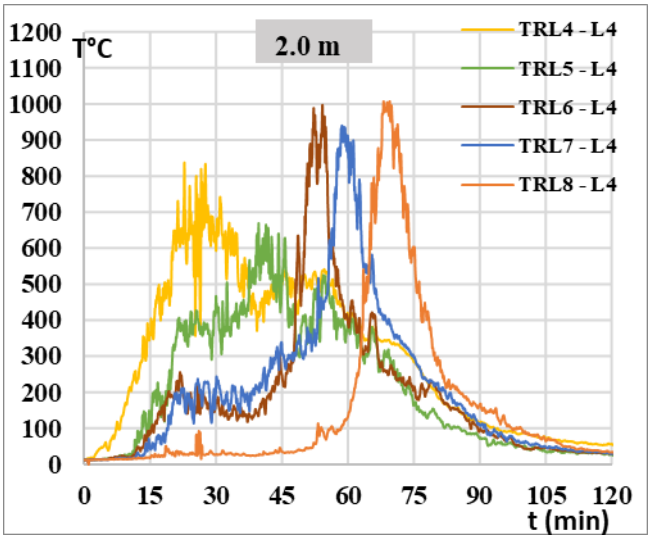

(d)

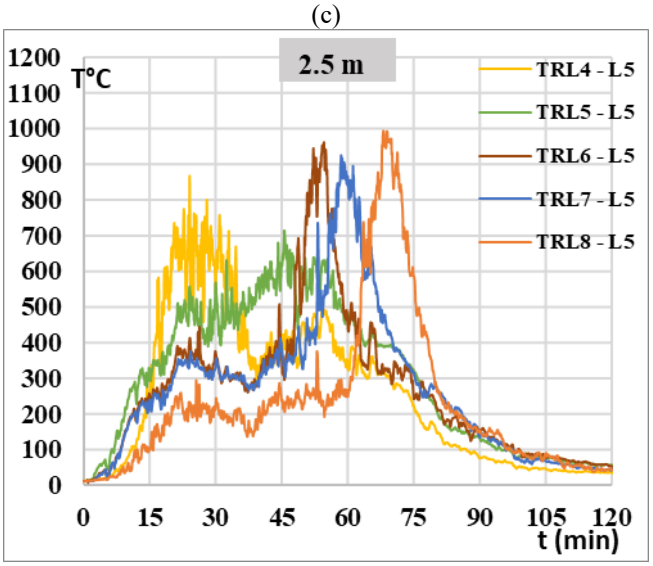

(e)

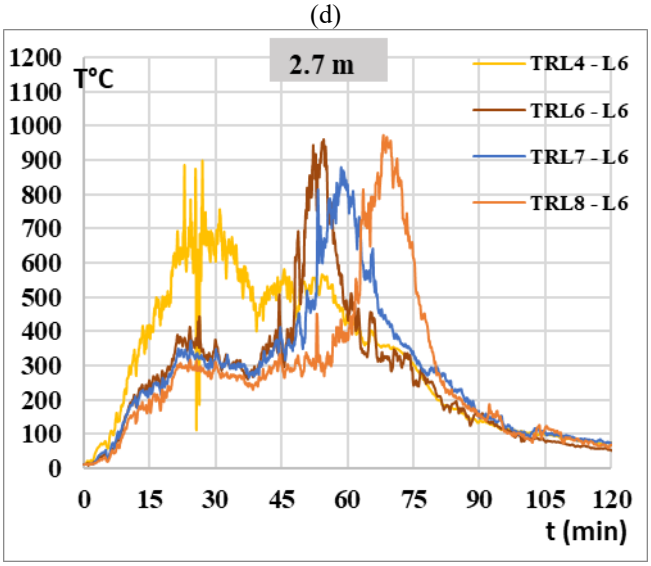

(f)

Figure 8: Evolution of gas temperatures in TRL-4 through TRL-8 at 5 different levels

3.3 Temperatures recorded int the Steel Structure

As stated previously, temperatures during the test were recorded in the selected beams and dummy columns. In this paper the columns and beams along gridline ② and ③ positioned between gridlines Ⓑ and Ⓒ have been selected for data presentation purposes. The selected columns and beams are adjacent to thermocouple trees TRL-5 and TRL-7, refer to Figure 3 (a). The test data is presented in terms of the recorded temperatures at different thermocouple positions shown earlier in Figure 3 (d) and (e). During the test, it was observed fire was concentrated near TRL-5 and TRL-7 after around 40 and 60 minutes respectively, as it can be observed on the graphs from Figure 9. The temperatures recorded in the compartment adjacent to the selected columns and beams, using thermocouple trees TRL-5 and TRL-7, are presented in Figure 9 (a) and (b), respectively. The temperature rise at higher levels L5 and L6 initiates earlier as compared to that at the lower levels. The temperature rise at L4 is earlier as compared to the remaining lower levels while it is

slower in comparison with levels L5 and L6. This is due the hot gases rising in the compartment, establishing in the upper part. For the bottom three levels, the increase in temperature is rapid as temperatures rises from 100°C to 1000°C within a few minutes as seen in Figure 9, translating the direct contact with the flames. For TRL-5, thermocouple provided at L6 was faulty, hence data is not included in Figure 9 (a).

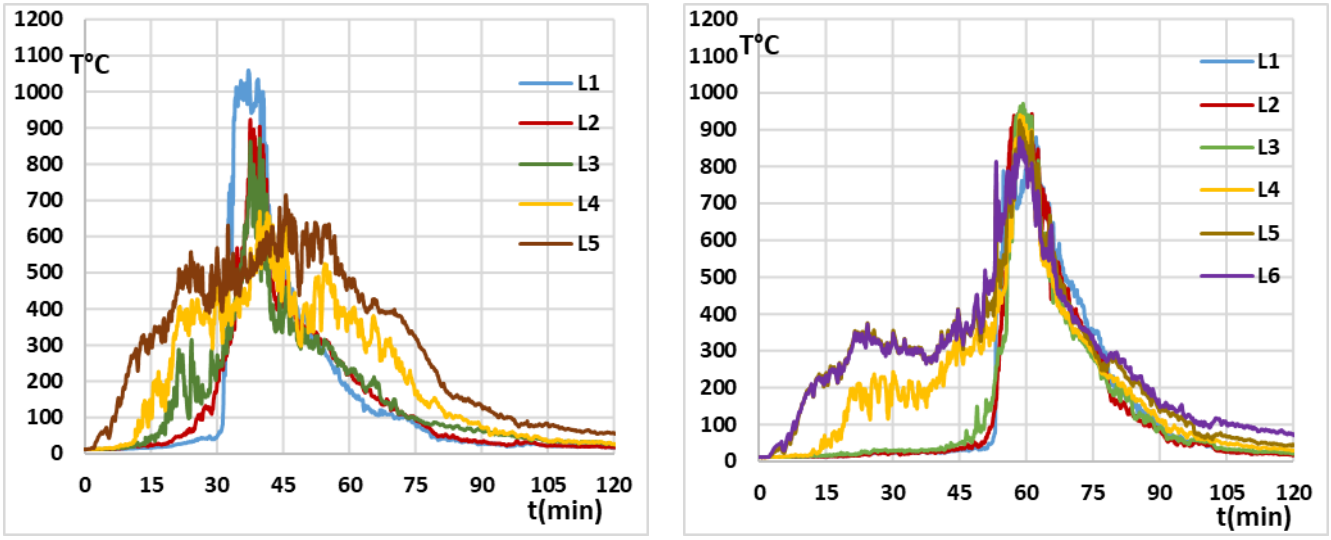

(a) (b)

Figure 9: Gas temperatures recorded at, (a) TRL-5; (b) TRL-7

3.3.1 Temperatures recorded in the steel columns

The temperatures recorded in the flanges and the web of the steel columns adjacent to TRL-5 and TRL-7 at all levels are presented in Figure 10. The label "LHS-F" corresponds to the flange closer to gridline Ⓒ (i.e. thermocouple numbers 1, 4, 7, 10, 13 in Figure 3 (d)) "WEB" corresponds to the web (i.e. thermocouple numbers 2, 5, 8, 11, 14 in Figure 3 (d)) and "RHS-F" corresponds to the flanges closer to gridline Ⓑ (i.e. thermocouple number 3, 6, 9, 12, 15 in Figure 3 (d)). During the test, some thermocouples were found faulty, these have not been included in Figure 10. The temperatures at L1 start to increase after 30 minutes for column adjacent to TRL-5 while the same for column adjacent to TRL-7 start after 55 minutes from the start of the test. For column adjacent to TRL-5, temperatures at L2 increase after 17 minutes while the same at L3 and L4 the rise in temperature initiates after 15 and 12 minutes respectively from the start of the test as shown in Figure 10 (b), (c) and (d) respectively. Similarly, for column adjacent to TRL-7, the temperatures at L2 rise after 52 minutes from ignition while those at L3 and L4 rise after 20 and 15 minutes as seen in

shown in Figure 10 (b), (c) and (d) respectively. For column near TRL-7, the rise in temperature at L4 for first 15 minutes is slow while it rises significantly as the wooden fuel near the column starts to burn. The temperatures recorded across the section of the columns at each level can be considered as uniform. At L5, the rise in temperature starts after a few minutes from the start of the test for both columns as shown in Figure 10 (e). It is interesting to see that for lower levels, the ascending part of the curve is steeper as compared to the descending branch. Further, the temperature recorded in the columns have similar profiles to the gas temperatures recorded in the adjacent columns provided earlier in Figure 9.

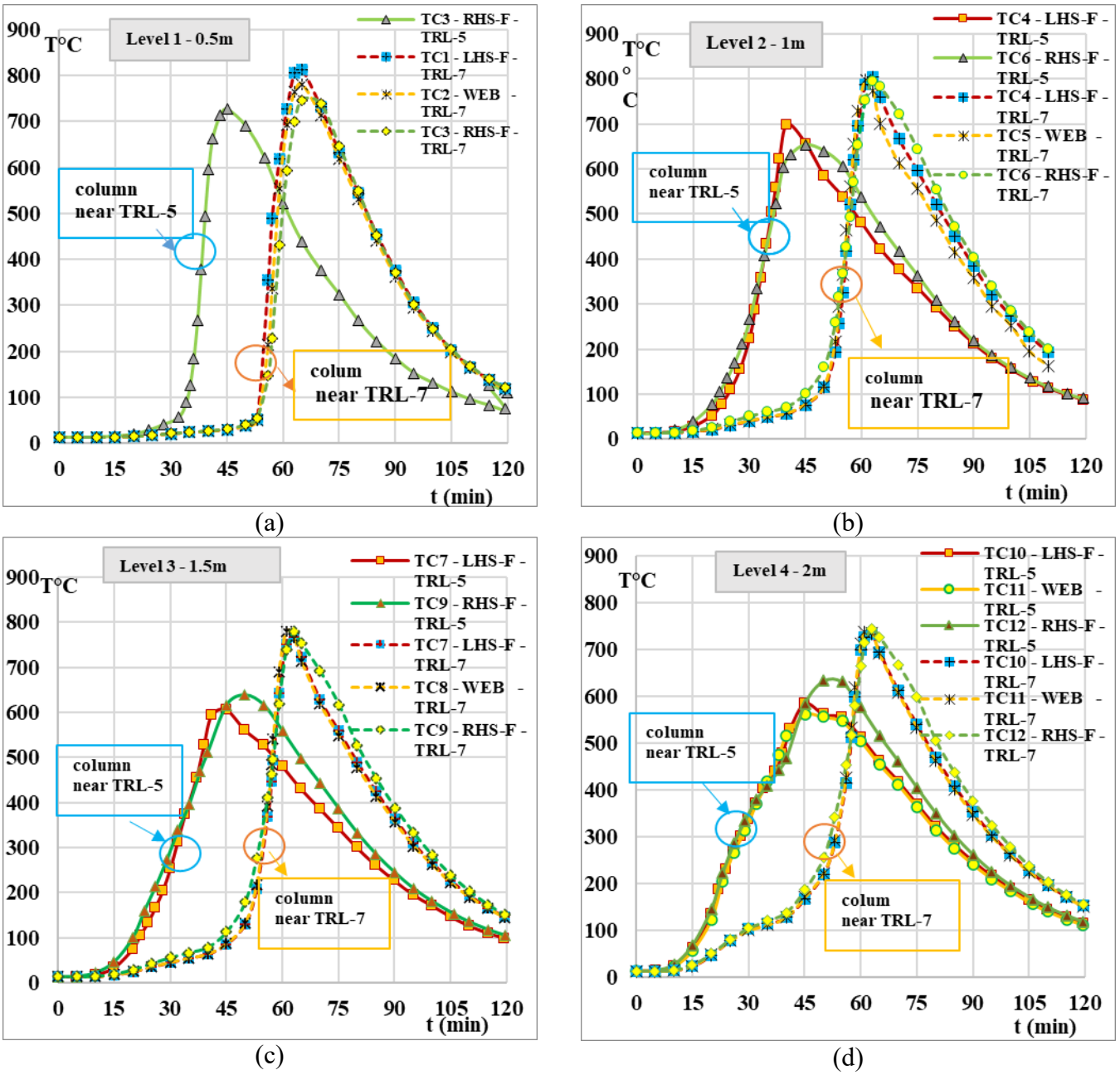

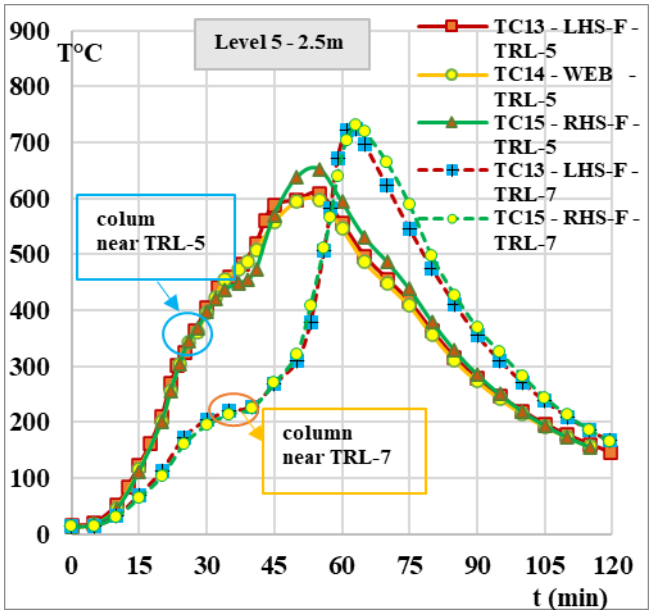

(e)

Figure 10: Evolution of steel temperatures in steel columns C11 adjacent to TRL-5 and TRL-7 at, (a) Level 1; (b) Level 2; (c) Level 3; (d) Level 4; (e)Level 5

The Figure 11 presents the temperature distribution along the height of the steel columns adjacent to TRL-5 and TRL-7 at 40 minutes and 70 minutes. For the column adjacent to TRL-5, it can be seen from Figure 11 (a) that at 40 minutes from ignition, the recorded steel temperatures are non-uniformly distributed along its height. At this time, the column is engulfed into the fire and higher temperatures are measured at its lower part. The bottom part of the column reaches 600ºC, while 520ºC and 470ºC are recorded at mid-height and closer to the ceiling level, respectively. At 70 minutes from the test, when the fire travels ahead and away from the column adjacent to TRL-5, high temperatures are maintained at L4 and L5 (at 2 and 2.5 meters) but temperatures at lower levels (at L1, L2 and L3) are relatively low with an average temperature of 410ºC.

In case of the column positioned adjacent TRL-7, it can be seen in Figure 11 (b) that at 40 minutes fire duration (i.e., when the flames have not reached the column yet): steel temperatures are quite low. At 70 minutes, steel temperatures exceed 700°C at lower levels (L1 and L2) while the temperatures at higher levels are approximately 650°C (at L3, L4 and L5). Such transient heating of the columns (and decrease of steel mechanical properties) should be considered when analysing the stability of a structure subjected to travelling fires.

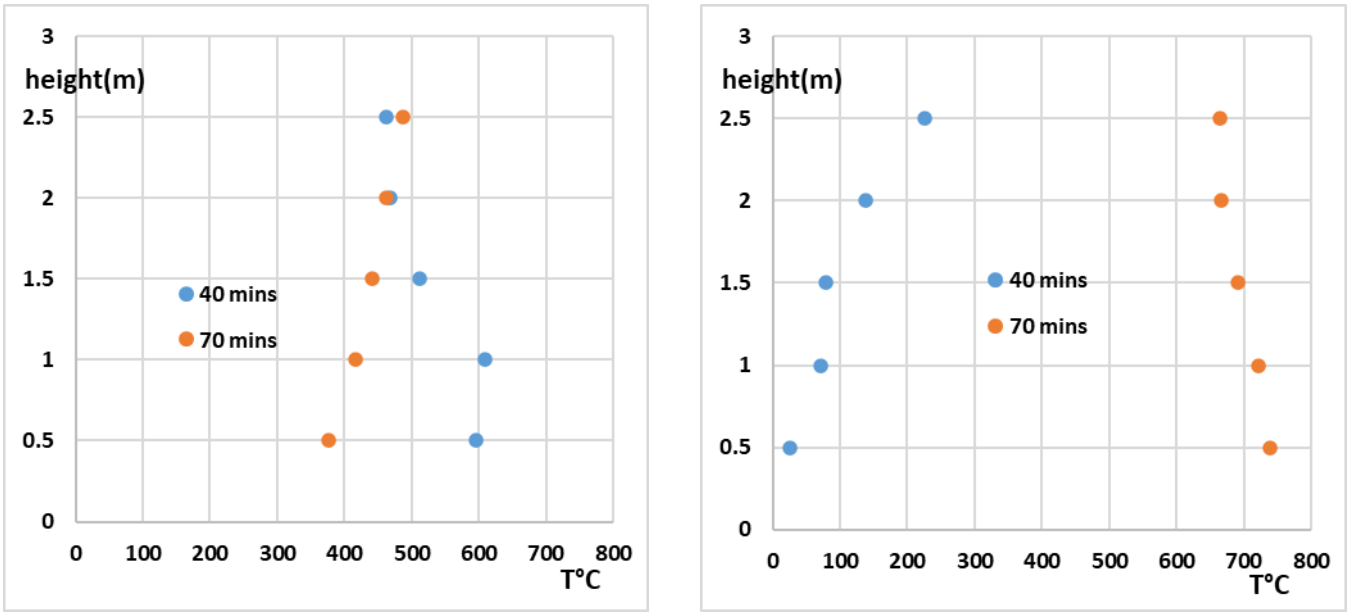

(a) (b)

Figure 11: Temperatures recorded at different levels in steel columns C11 adjacent to, (a) TRL-5; (b) TRL-7

3.3.2 Temperatures recorded in the steel Beams

The selected beams were instrumented with a set of three thermocouples, one on each flange and one on the steel web, as shown previously in Figure 3 (e). The beams considered for data presentation purposes consist of hot rolled steel profiles HEA-160 provided along gridlines ② and ③ located between gridlines Ⓑ and Ⓒ. The gas temperatures in the compartment adjacent to the thermocouples in the beam were recorded at L5 and L6 (in TRL-5 and TRL-7 given earlier in Figure 9). For each beam, the temperatures are presented using three curves, B16 - BF corresponds to bottom flange, B17 – WEB corresponds to the middle of the web while B18 – TF corresponds to the top flange in Figure 12. Temperatures in the beam adjacent to TRL-5, being closer to the point of ignition, increase significantly after 12 minutes from the start of the test. However, for beam adjacent to TRL-7, a slower increase is recorded until the 45th minute. Once the travelling fire gets closer, a sharp increase in temperature is recorded as seen in Figure 12. It can also be observed that the decrease in temperatures starts in the beam adjacent to TRL-5 earlier than the beam adjacent to TRL-7 as the fire travels ahead towards the fore end of the test compartment. It is interesting to note that the temperatures measured in the bottom flange, web and the top flange are non-uniform: the temperatures in the top flange are significantly lower as compared to those recorded in the bottom flange. The maximum steel temperatures reached in the bottom flange, the web and the top flange are 605°C, 600°C and 500°C respectively for beam adjacent to TRL-5. Similarly, the maximum temperatures recorded in the

bottom flange, web and top flange for beam adjacent to TRL-5 are 700°C, 675°C and 595°C respectively as seen in Figure 12. These results not only show non-uniform temperatures in the test compartment, but they also highlight the transient heating of the surrounding structure for travelling fires.

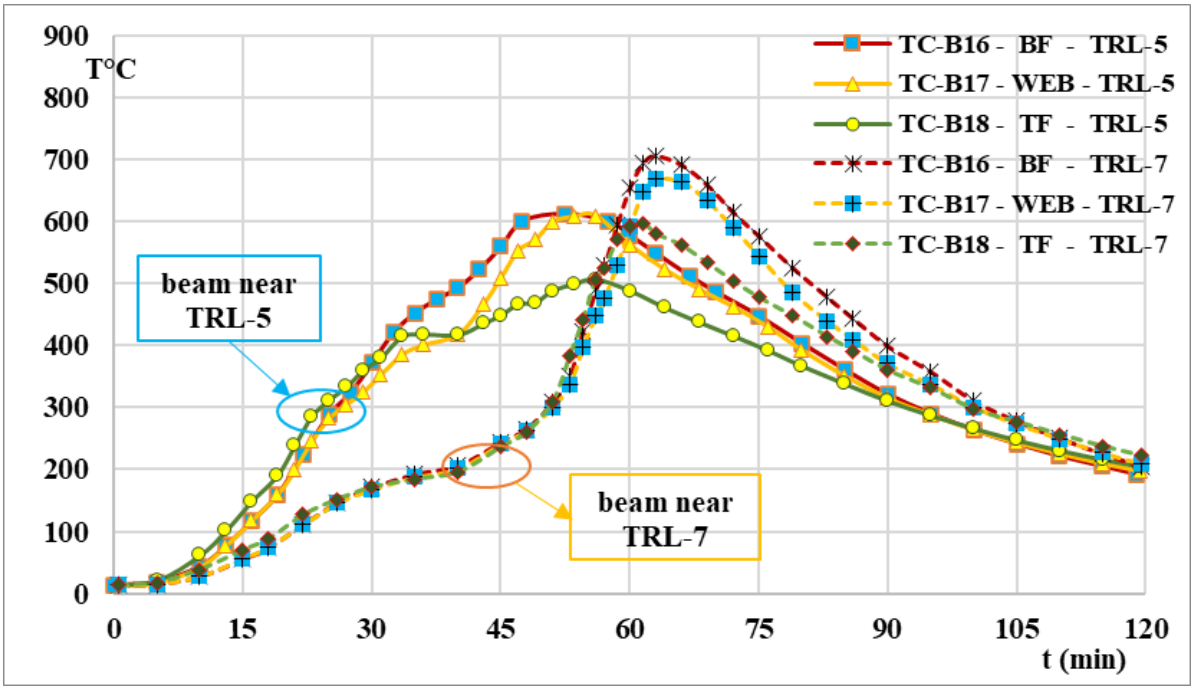

Figure 12: Evolution of temperatures in beams along gridlines ② and ③ adjacent to TRL-5 and TRL-7

3.4 Mass Loss of the Burning Fuel

The mass loss data recorded during the test is presented in Figure 13 (a). As observed during the test, a decrease in the mass of the fuel wood supported on the platform is seen once it starts to burn fire after 37 minutes from ignition. After 39 min onwards until the 58th minute, a uniform decrease in the wooden fuel mass is recorded. After 58 min from ignition, a slow reduction in the mass loss is recorded due to non-uniformity of the burning fuel. The mass loss recordings also comply with the observations made during the test where most of the fuel wood provided on the platform was consumed after 64 minutes.

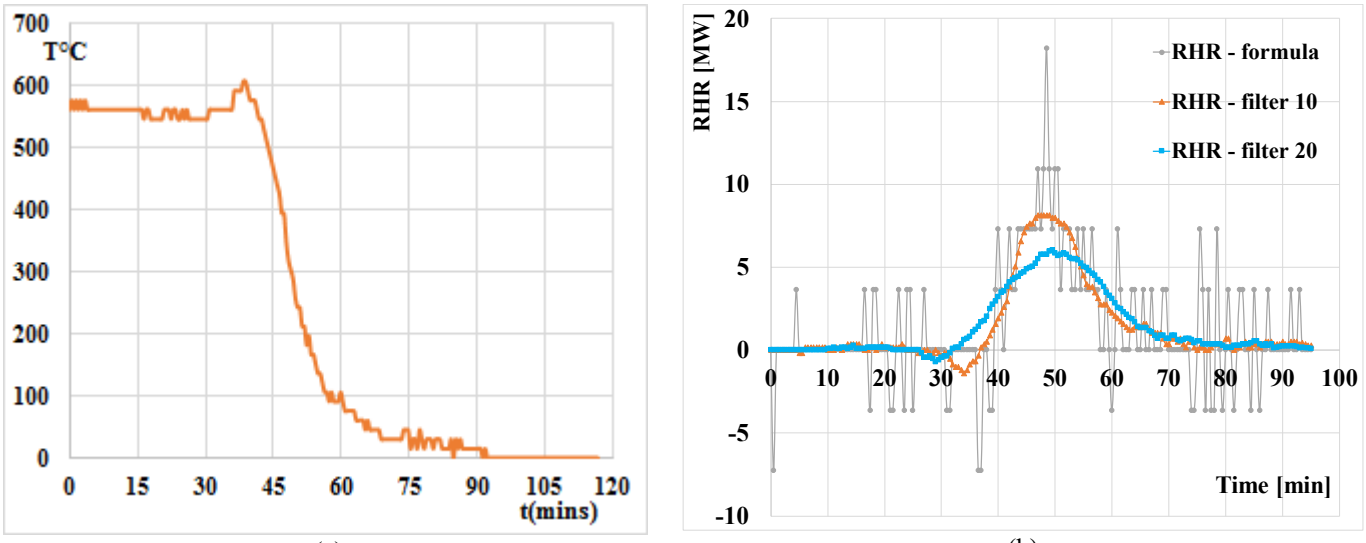

(a) (b)

Figure 13: (a) Recorded mass loss; (b) Approximation of the RHR, derived from the mass loss measurements

The mass loss rate [kg/s] is the variation of the solid fuel mass during the combustion process. It is possible to deduce the rate of heat release from the mass loss rate, since these two parameters are linked by the equations (1) and (2), H_u being the net calorific value of the fuel [MJ/kg] and m being the combustion factor (considered equal to 0.8, following Eurocode 1). To evaluate the mass loss rate from the continuously measured mass, a backward finite difference scheme must be applied, which requires the definition of a fixed time step. There is no unique correct value for this time step; but the following consequences should be considered: a more important time step implies a smoother curve, while a less important time step translates in a more precise way the measurements but might provide unrealistic peaks (noise and outliers). Finally, a time step Δt = 60 seconds was considered as an acceptable compromise.

$$RHR(t) = H_u.m.MLR(t) \quad (1)$$

$$RHR(t) = -H_u.m.\frac{dm}{dt} = -H_u.m.\frac{\Delta m}{\Delta t} \quad (2)$$

As the mass loss rate is the derivative of an experimental signal, noise and outliers (for example negative values) are quickly generated. One method to cope with this is to filter the curve using, for example, a Savitzky–Golay filter. This digital filter that can be applied to a set of digital data points for the purpose of smoothing the data, that is, to increase the precision of the data without distorting the signal tendency. This is achieved, in a process known as convolution, by fitting successive sub-sets of adjacent data points with a low-degree polynomial. The simplest form of this approach, called running average,

consists in computing the average for each subset. This approach is commonly used with time series data to smooth out short-term fluctuations and highlight longer-term trends or cycles. The RHR [kW] obtained by derivative of the mass loss using a time step of 60 seconds, the filtered RHR obtained with smoothing parameters of 10 and 20 are depicted in Figure 13 (b). The filtered RHR with parameters 10 and 20 show maxima values of 8140 kW and 5850 kW, respectively. It must be noted that some discrepancies can be noticed with wooden fuel load, at the end of the combustion process. Indeed, the heat of combustion of wood is not perfectly constant: it is higher at the end of a test when only embers are left.

4 CFD SIMULATIONS (SIMPLIFIED APPROACH)

Several CFD simulations were launched with FDS software to calibrate the model representing the large-scale tests. These CFD simulations consider a simplified representation of the continuous fire load consisting of discrete volumes based on a regular arrangement [16]. Simplification was targeted, as modelling the exact wood stick size in CFD requires a very fine mesh and therefore a very significant computational time for real building dimensions. The proposed approach can allow for both an acceptable representation of the travelling fire in terms of fire spread and steel temperatures while being less computationally demanding than modelling the exact geometry of the fire load, making it more desirable for practical applications. The modelled compartment is represented in Figure 14. The steel temperatures which were recorded at five different levels in the column next to TRL-7 are compared with numerical results: In a first simplified step, the CFD output 'THERMOCOUPLE' was used to evaluate the related steel temperature using the incremental formula from EN1993-1-2 [15]. In a second and more complex step, a coupling between CFD (FDS software) and FE (SAFIR® software version 2019b0 [17]) was used. Radiative intensities and gas temperatures calculated by FDS have been used by SAFIR® to calculate the temperatures in the steel column. The Figure 15 and Figure 16 present the steel temperatures in column close to TRL-7, from L2 (1.0 m from the floor level) to L5 (2.5 m from the floor level). The inspection of the temperatures obtained via FDS-SAFIR (see label “SAFIR” on Figure 15 and Figure 16) shows that the global profile versus time is well captured, even though steel temperatures from lower levels are higher than the ones measured. More details are provided in Charlier et al. [16].

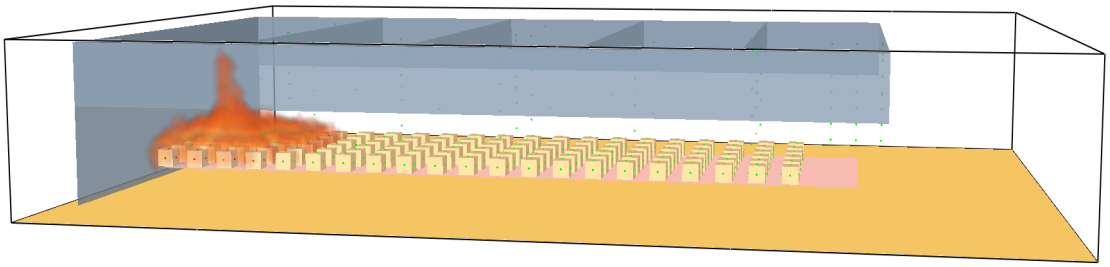

Figure 14: Modelled compartment in FDS (example with 0.32 m size cubes)

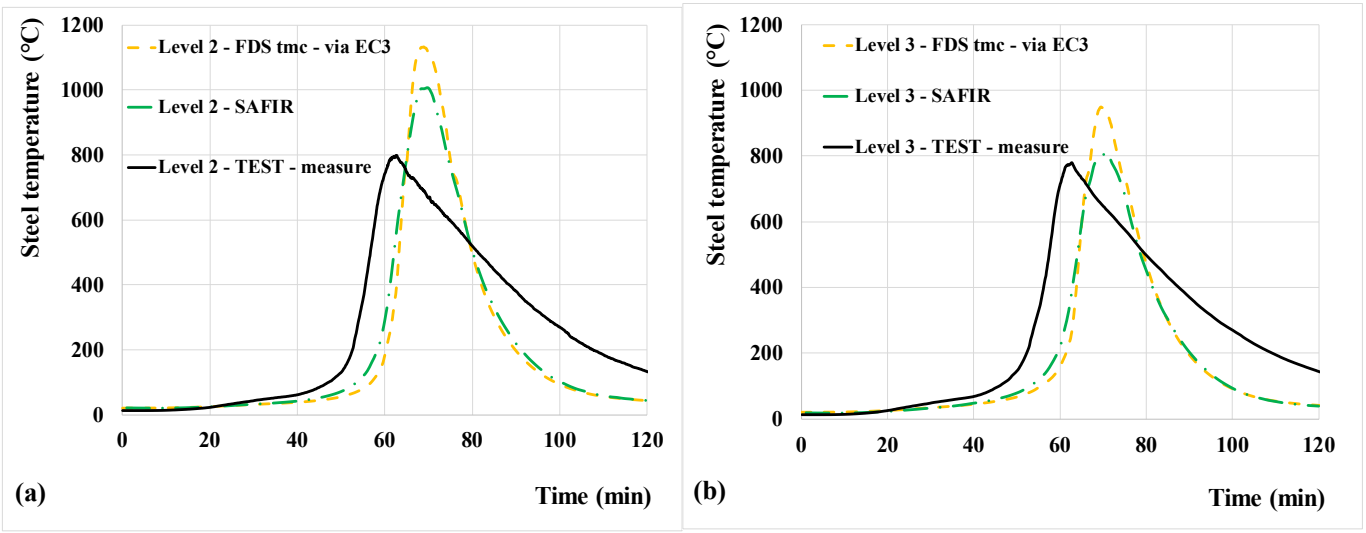

Figure 15. Steel temperatures in column close to TRL7 during test n°1 (a) at level 2; (b) at level 3 [14]

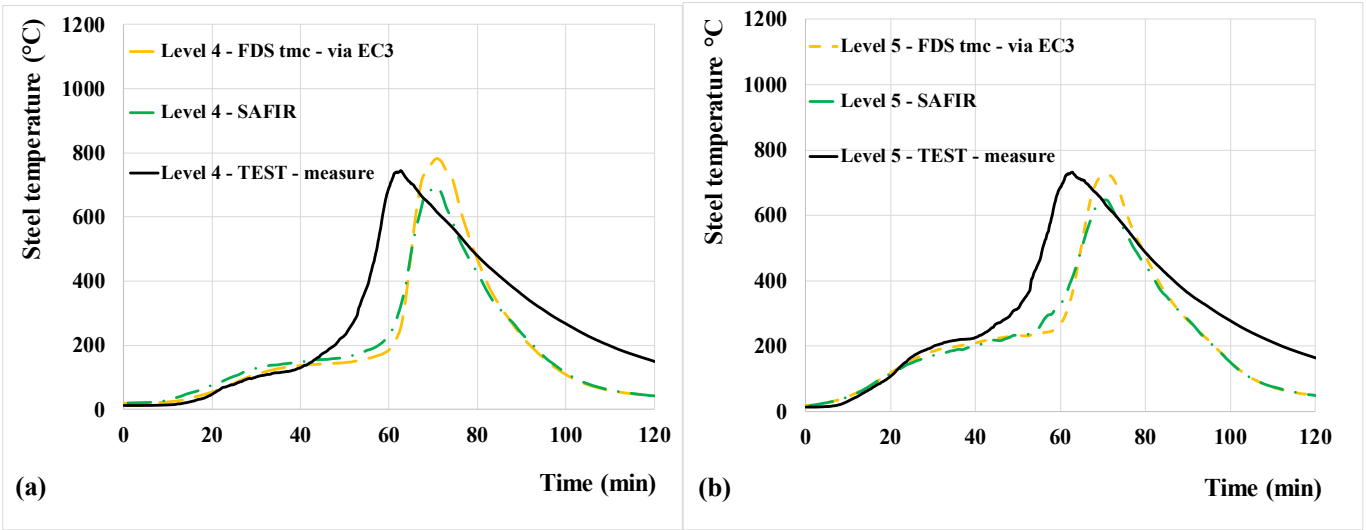

Figure 16. Steel temperatures in column close to TRL7 during test n°1 (a) at level 4; (b) at level 5 [14]

5 CONCLUSIONS

Three large scale natural fire tests were performed in a building with large dimensions. A fire load representative of an office building, defined according to a well-established methodology was used for the

three tests, only the ventilation was varied to assess its influence on the fire behaviour. The main objectives of this experimental campaign were to understand in which conditions a travelling fire develops, as well as how it behaves and impacts the surrounding structure. Instrumentation was installed to measure compartment temperatures, surface temperatures, heat fluxes and temperature in the steel columns, and beams. This article presented details only of the first fire test in terms of gas temperatures recorded in the central part of the compartment, along its length. The details related to the maximum flame thickness, steel temperatures in selected central beams and columns, as well as mass loss data were also provided. Following are major conclusions from the travelling fire test.

- For the fire initiating at a single point, its developing phase consists of increase in the volume of fire in all directions making a circle around the point of ignition. Once the fire is well developed, it continues to travel along the fuel bed. In the case of the test conducted during this research, the fire travelled in the forward direction towards the fore end of the compartment. However, the fire could travel in any direction depending upon the availability of the fuel.
- The rise in temperatures at higher levels starts at the initial stages of test while the rise at lower levels starts once the fuel wood starts to burn locally. The temperatures in the compartment were found to be dependent on the positioning of the travelling fire. The parts of the compartment around the fire are hotter while the parts away from the fire were at lower temperatures.
- The results obtained from the fire test demonstrated the non-uniform temperature distribution, leading to the heating of the nearby structural steel elements, resulting in a reduction of individual members' resistance, which could influence the global structural stability. Such transient heating of the columns should be considered when analysing the stability of a structure subjected to travelling fires.
- All the connections and steel members performed well and showed no signs of failure during the fire test.
- The results obtained from the CFD modelling were quite similar to those obtained during the test with the main difference being the maximum temperatures. The steel temperatures obtained via CFD

modelling generally displayed a good agreement with the test but underestimated the descending branch. Further, the temperatures predicted near the fuel were also high.

ACKNOWLEDGMENT

This work was carried out in the frame of the TRAFIR project with funding from the Research Fund for Coal and Steel (grant N°754198). Partners are ArcelorMittal, Liège University, the University of Edinburgh, RISE Research Institutes of Sweden and the University of Ulster. The authors also wish to acknowledge the supporting of companies Sean Timoney & Sons Ltd, FP McCann Ltd, Saverfield Ltd and Crossfire Ltd.

REFERENCES

1. J. Stern-Gottfried, G. Rein (2012). *Travelling fires for structural design – Part I: Literature review.* Fire Safety Journal 54. pp 74- 85.
2. EN1991-1-2 (2002). Eurocode 1: Actions on structures – Part 1- 2: General Actions on structures exposed to fire. CEN, Brussels.
3. R. G. Gann, A. Hamins, K. McGrattan, H. E. Nelson, T. J. Ohlemiller, K. R. Prasad, and W. M. Pitts, (2013) Reconstruction of the fires and thermal environment in World Trade Center buildings 1, 2, and 7, Fire Technol., vol. 49, pp. 679–707.
4. I. Fletcher, A. Borg, N. Hitchen, and S. Welch, (2005) Performance of concrete in fire: A review of the state of the art, with a case study of the Windsor Tower fire," in 4th International Work- shop in Structures in Fire, pp. 779–790.
5. D. M. Zannoni, J. G. H. Bos, D. K. E. Engel, and P. dr. U. (2008) Rosenthal, Brand bij Bouwkunde.
6. Dai X, Welch S and Usmani A (2017) A critical review of 'travelling fire' scenarios for performance-based structural engineering. Fire Safety Journal 91: 568–578.
7. G. Rein, X. Zhang, P. Williams, B. Hume, A. Heise, A. Jowsey, B. Lane, and J. L. Torero, (2007) Multi-storey fire analysis for high- rise buildings, in Proceedings of the 11th International Inter- flam Conference, London, UK, pp. 605–616.
8. K. Horová, T. Jána, F. Wald (2013). Temperature heterogeneity during travelling fire on experimental building. Advances in En- gineering Software 62-63. pp 119-130.

9. J.P. Hidalgo, A. Cowlard, C. Abecassis-Empis, C. Maluk, A.H. Maj- dalani, S. Kahrmann, R. Hilditch, M. Krajcovic, J.L. Torero (2017). An experimental study of full-scale open floor plan en- closure fires. Fire Safety Journal 89. pp 22-40.
10. J. P. Hidalgo, T Goode, V. Gupta, A. Cowlard, C Abecassis-Empis, J. Maclean, A. Barlett, C. Maluk, J.M. Montalva, A. F. Osorio, J. L. Torero (2019). The Malveira fire test: Full-scale demonstration of fire modes in open-plan compartments. Fire Safety Jour- nal vol.108 No 102827.
11. A. Gamba, M. Charlier, J.M. Franssen (2020). Propagation tests with uniformly distributed cellulosic fire load. Fire Safety Journal 117, 103213.
12. J. Degler, A. Eliasson, A. Anderson, D. Lange, D. Rush (2015). A- priori modelling of the Tisova fire test as input to the experimental work. Proc. 1rst Int. Conf. on Struct. Safety under Fire & Blast, Glasgow, UK.
13. M. Charlier, A. Gamba, X. Dai, S. Welch, O. Vassart, J.M. Franssen (2020). Modelling the influence of steel structure compartment geometry on travelling fires. Proceedings of the Institution of Civil Engineers - Structures and Buildings. https://doi.org/10.1680/jstbu.20.00073.
14. Rackauskaite, E., Hamel, C., Law, A. & Rein, G. (2015) "Improved formulation of travelling fires and application to concrete and steel structures", Structures 3:250–260
15. CEN (European Committee for Standardization) (2005), "EN 1993-1-2: Eurocode 3: Design of steel structures - Part 1-2: General rules - Structural fire design", Brussels, Belgium.
16. Charlier, M., Glorieux, A., Dai, X., Alam N., Welch, S., Anderson, J, Vassart, O, Nadjai, A. (2021), "Travelling fire experiments in steel-framed structure: numerical investigations with CFD and FEM, accepted by the Journal of Structural Fire Engineering
17. Franssen, J.-M., Gernay, T. (2017), "Modeling structures in fire with SAFIR®: Theoretical background and capabilities", *Journal of Structural Fire Engineering 8(3)*, pp.300-323. https://doi.org/10.1108/JSFE-07-2016-0010